PHYSICAL REVIEW B **66**, 081310(R) (2002)

Fine structure of trions and excitons in single GaAs quantum dots

J. G. Tischler, A. S. Bracker, D. Gammon, and D. Park
Naval Research Laboratory, Washington DC 20375-5347
(Received 1 July 2002; published 30 August 2002)

Trions and excitons, localized laterally in quantum-dot-like potentials in GaAs quantum wells, were studied by magnetophotoluminescence spectroscopy as a function of magnetic field strength and orientation. Single-trion spectroscopy was demonstrated using high spatial resolution. We present a comparative study of the fine structure of single localized excitons and trions.

DOI: 10.1103/PhysRevB.66.081310 PACS number(s): 78.67.Hc, 73.21.−b, 71.35.−y

Although the negatively charged trion in semiconductors was originally predicted in 1958 by Lampert,[1] a proper identification of the X^- was not achieved until the early 1990s in remotely doped high-quality quantum-well (QW) structures.[2–4] Since then, extensive work has been carried out on the two-dimensional (2D) X^- in wide quantum wells,[2–10] and more recently on the 0D X^- in QD's.[11] In many of these studies a recurrent and sometimes controversial question keeps popping up: how localized are the excitonic states and how does confinement affect the Coulomb interaction.[3–7] It has been suggested that the 2D X^-s may be localized and their spectra broadened by potential fluctuations generated by the ionized donors in the barriers.[3,6] Another source of localization[7] is provided by interface fluctuations, which are known to play an important role in the localization of excitons (X's).[12] Here we demonstrate the complete *quantum confinement* of a trion by using monolayer-high islands at the interfaces of narrow quantum wells to confine trions in three-dimensional QD-like potentials. This allows us to apply the methodology of single QD spectroscopy to probe individual trions. In so doing we identify distinctive signatures in the fine structure of their magneto-optical spectra. The latter provides a characterization and understanding of the singlet state of the trion transition.

The samples utilized in these studies were grown by molecular beam epitaxy on semi-insulating GaAs(100) substrates. The structure consists of five quantum wells of different well widths (nominally 2.8, 4.2, 6.2, 8.4, and 14.0 nm) surrounded by 40-nm $Al_{0.3}Ga_{0.7}As$ barriers. The quantum wells were grown with two-minute growth interrupts at the interfaces to allow large monolayer-high islands to develop.[12] We incorporated electrons in each of the quantum wells by silicon doping 3 nm of the barriers 10 nm above the top well/barrier interface. Ensemble and single QD photoluminescence (PL) were excited with an argon laser at 514.5 nm and detected with a triple spectrometer and a charged-coupled device detector in a split-coil superconducting magnet. Individual QD's were excited and detected through submicron diameter apertures in an aluminum shadow mask patterned on the sample surface.[12]

Figure 1 shows typical ensemble PL spectra of excitons and trions for four modulation-doped GaAs quantum wells with different widths (L_z). The widest well (14 nm) shows two well-resolved peaks identified in earlier work as the exciton and trion with a separation of 1.2 meV, in good agreement with previous reports.[2–8] With decreasing well width this splitting increases to 3 meV at 2.8 nm, as shown in the inset to Fig. 1. For all well widths the trion peaks disappear quickly with increasing temperature (dotted-line spectrum). At the same time well-resolved monolayer splittings develop in both the exciton and trion peaks. These monolayer splittings, which grow at a much faster rate, provide a measure of the lateral confinement.[12] As seen in the inset the lateral confinement becomes much larger than the trion ''binding energy'' and the trions become laterally confined in QDs in sufficiently narrow quantum wells. Although the qualitative behavior of the binding energy as a function of well width agrees with theoretical predictions,[7–8] the binding energy for the narrowest quantum well is at least twice the predicted value.[7–8] As pointed out by Riva *et al.*,[7] this discrepancy is likely due to the lateral confinement of the X^- and X, which affects the Coulomb interactions.

Associated with the large increase in lateral confinement is a rapid increase in linewidth for both the exciton and trion ensembles. This inhomogeneous spread in the trion energies allows us to spectrally resolve individual trions and excitons using high spatial resolution.

In the rest of the paper we present a detailed magneto-PL study of a single representative trion in the 2.8-nm quantum

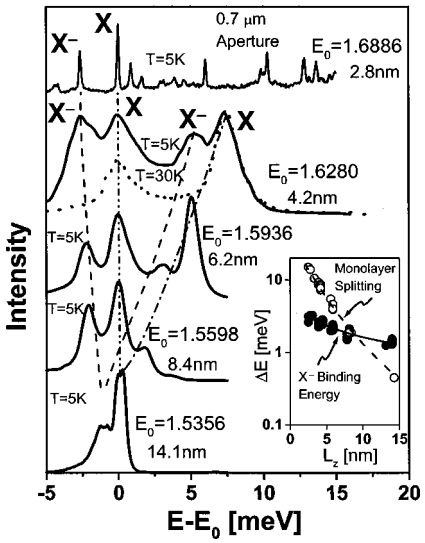

FIG. 1. Ensemble PL spectra for several quantum well widths and one spectrum through a 0.7-μm-diameter aperture. Inset: well width dependence of the binding energy of the trion and monolayer splittings.

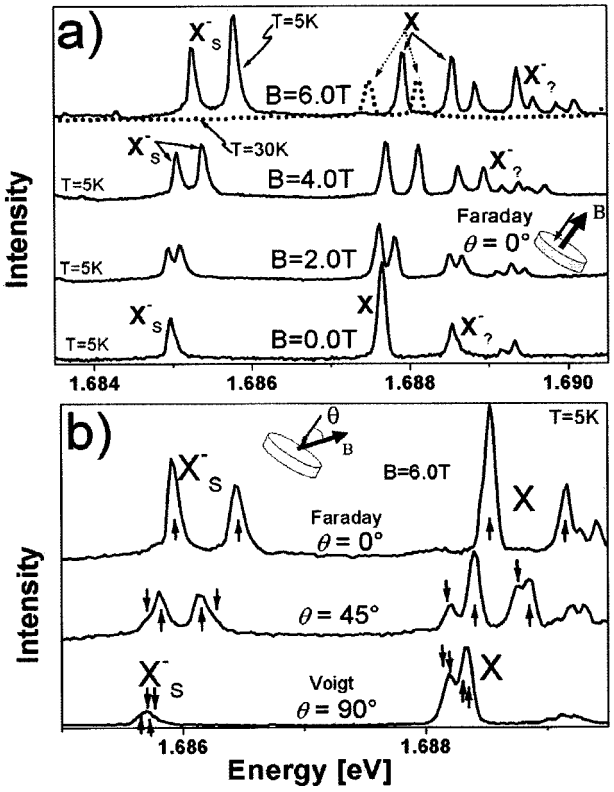

FIG. 2. Single dot magneto-PL in the (a) Faraday geometry, and (b) at $B=6$ T as a function of the polar angle (θ). A comparison between the spectra at $T=5$ and 30 K reveals the absence of the X_s^-. The redshift of the exciton at $T=30$ K arises from a decrease in band gap at increased temperature. Upward (downward) arrows indicate the bright (dark) related transitions.

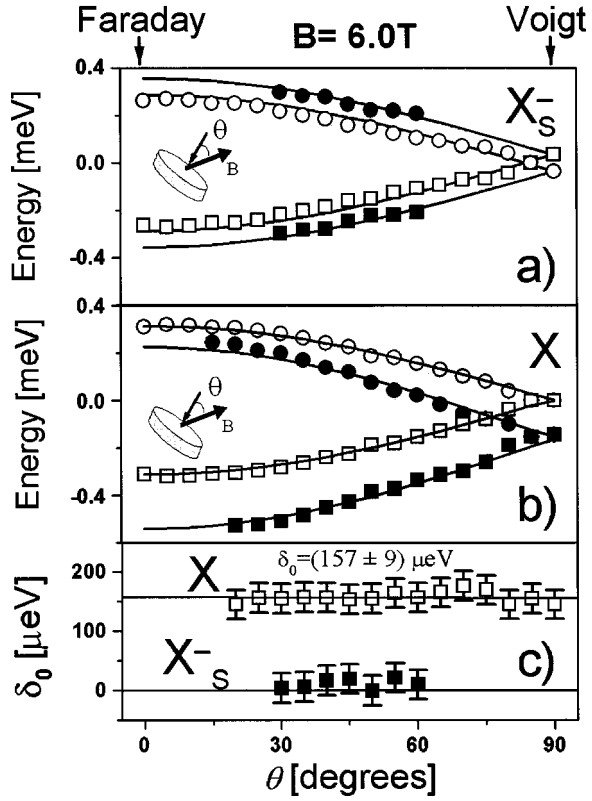

FIG. 3. The dependence on polar angle (θ) of the dark (solid symbols) and bright-related (open symbols) transitions for the (a) trion singlet (X_s^-) and (b) exciton (X) at 6.0 T. (c) Fine structure parameter (δ_0) for the exciton (open symbols) and trion (solid symbols).

well through a 0.7-μm aperture. Shown in Fig. 2(a) are PL spectra obtained in the Faraday geometry (i.e., magnetic field along the z axis and perpendicular to the quantum-well plane) at several field strengths. As can be seen from this figure, in the absence of a magnetic field the PL spectra are characterized by two predominant transitions that we identify as exciton (X) and trion singlet (X_s^-) recombination transitions from the lower monolayer. As the temperature is increased several lines rapidly decrease in intensity. By 30 K all lines related to the trion disappear as shown in Fig. 2(a) (dotted-line spectrum). This effect is due to the ionization of one of the electrons from the three-particle trion system, which is consistent with previous results on the 2D X^-.[2–3] With the field applied along the z axis, all lines split into doublets with similar g factors.

Figure 2(b) shows PL from the same aperture at a constant field of 6.0 T at several polar angles (θ), defined as the angle between the z-direction and the magnetic field [Fig. 2(b), inset]. When the magnetic field is applied in the quantum well (x-y) plane ($\theta=90°$, Voigt geometry), both transitions, X_s^- and X exhibit quite different behaviors. In the case of the X, the so-called dark-related transition(s) grow at lower energy as the magnetic field is increased.[13,14] This is clearly not the case for the X_s^-, which does not exhibit a well-resolved lower-energy transition(s). Furthermore, for other polar angles [see, for example, data at 45° in Fig. 2(b)], the X and X_s^- show two dark and two bright-related transitions with distinctive signatures. These transitions are indicated with upward arrows for the bright-related transitions, while downward arrows indicate dark-related transitions. A summary plot for the X and X_s^- fine structure as a function of θ is plotted in Figs. 3(a) and 3(b), respectively, after subtracting the diamagnetic shift. Open symbols are the bright-related transitions while solid symbols indicate the dark-related transitions.

In order to understand this behavior it is necessary to explore the spin states of the X and X^- in a QD as a function of magnetic field (Fig. 4). Both entities X and X^- are formed by electrons ($S_z=\pm 1/2$) and heavy holes ($J_z=\pm 3/2$) strongly confined by the QW in the z direction and weakly confined in the lateral direction by interface fluctuations. The X is formed by one electron and one heavy hole; as a result, four states can be formed which are characterized by their angular momentum projections (M). The degeneracy of these four levels ($|M=\pm 1\rangle, |M=\pm 2\rangle$), which recombine into the vacuum state ($|0\rangle=|M=0\rangle$), is broken even at zero magnetic field due to the exchange energies (δ_0, δ_b, and δ_d).[12–18] On the other hand the X^- is formed by two electrons and a hole, and therefore eight states can be formed. Two of these states are the so-called singlet states ($|X_S^-\rangle = |M=\pm 3/2\rangle$) where both electrons are in the lowest confined state of the QD, and their spins are opposite to each

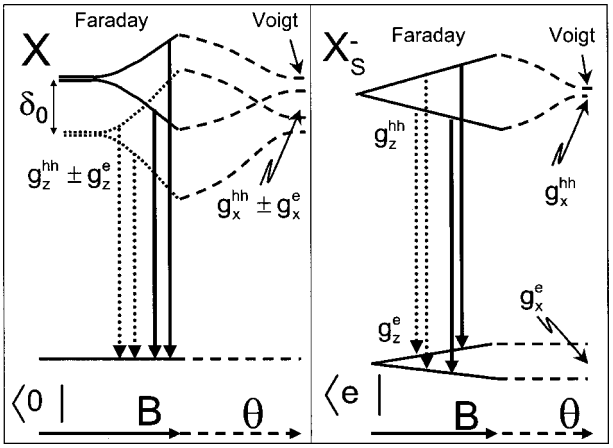

FIG. 4. Schematics of the excited and ground states involved in the exciton (X) and trion singlet (X_s^-) transitions studied as a function of magnetic field strength (B) in the Faraday geometry ($\theta = 0$), and as a function of orientation (θ) at constant B. The solid arrows indicate bright-related transitions while the dotted arrows indicate dark-related transitions.

other. Because of the pairing of these electrons no exchange energies are present for the singlet state. The other six states (triplet states, X_T^-) require an electron in a higher energy spatially confined state in the QD, and therefore located at much higher energy and not affecting the singlet states. Once the trion recombines, a single electron is left behind ($|e\rangle = |M = \pm 1/2\rangle$).

The X is fourfold degenerate, and its field dependence is determined by the exchange energies and g factors of the heavy hole and electron,[13–14] while the X_S^- is a doublet given only by the g factor of the heavy hole. Similarly, the final state of the X *transition* is unique and field independent, while the final state of the X_S^- *transition* is a doublet and depends only on the g factor of the electron (e). Once we consider all these states, it is easy to see that both entities will have four possible recombination channels as shown in Fig. 4. If we consider the optical selection rules ($\Delta M = 0, \pm 1$), we observe that in the Faraday geometry (and in the absence of a magnetic field) both X and X_S^- have two allowed transitions (solid lines) and two forbidden transitions (dotted lines). In any other case (including the Voigt geometry), the initial and final states are mixtures of $|M\rangle$ states, allowing all four transitions to be observed for both entities. In the Faraday and Voigt geometries, the expected g factors for the X *and* X_S^- are the same for both the bright (allowed) and dark (forbidden) transitions.

The main difference between the X and X_S^- fine structure is the absence of exchange energy in the case of X_S^-. For the X we find that δ_0 is approximately constant for a given well width: δ_0 is dominated by the QW width and the particular lateral size and shape of the QD has little effect. Therefore, the absence of a lower energy transition(s) in the Voigt geometry [Fig. 2(b)] is a clear identification of X_S^-, and confirms our initial assignment made on the basis of its temperature dependence and binding energy.

With this model it is possible to fit the measured X and X_S^- transitions as a function of the polar angle (θ) at a constant magnetic field (B) [Figs. 3(a) and 3(b)]. The Hamiltonian for the exciton can be written as

$$\hat{H}_X = \frac{\delta_0}{2}\hat{\sigma}_z^e\hat{\sigma}_z^h + \frac{\mu_B \mathbf{B}}{2}\cdot(\bar{\bar{g}}^e\cdot\hat{\sigma}^e + \bar{\bar{g}}^h\cdot\hat{\sigma}^h), \tag{1}$$

where the first term is due to the exchange and the second to the Zeeman interaction.[15–19] In this expression μ_B is the Bohr magneton and $\hat{\sigma}_i$ are the Pauli spin matrices. The g-factor tensor ($\bar{\bar{g}}$) has only diagonal terms in the reference coordinate system given by the symmetry axes of the QD, in our case the crystal axis [001], [110], and $[\bar{1}10]$.[13,14] The heavy hole is treated as a pseudospin using Pauli spin matrices with $\pm 3/2 \rightarrow \mp 1/2$.[17] We have neglected the other exchange terms (δ_b, δ_d) here, because they are smaller than the linewidths for this QD.[18]

In the case of the X_S^-, the Hamiltonian can be written as

$$\hat{H}_{X_S^-} = \frac{\mu_B \mathbf{B}}{2}\cdot\bar{\bar{g}}^h\cdot\hat{\sigma}^h = \frac{\mu_B\cdot B}{2}\begin{pmatrix} g_z^{hh}\cos\theta & g_x^{hh}\sin\theta \\ g_x^{hh}\sin\theta & -g_z^{hh}\cos\theta \end{pmatrix}, \tag{2}$$

g_z^{hh} is the heavy-hole g factor in the z direction, and g_x^{hh} is the heavy-hole g factor in the x-direction.

Similarly, the final-state Hamiltonian is

$$\hat{H}_e = \frac{\mu_B \mathbf{B}}{2}\cdot\bar{\bar{g}}^e\cdot\hat{\sigma}^e = \frac{\mu_B B}{2}\begin{pmatrix} g_z^e\cos\theta & g_x^e\sin\theta \\ g_x^e\sin\theta & -g_z^e\cos\theta \end{pmatrix}, \tag{3}$$

where g_z^e is the g-factor of the electron in the z direction and g_x^e is the electron in-plane g factor. After diagonalizing both matrices and taking all possible differences between the different eigenvalues, we obtain the expression for the X_S^- bright-related and dark-related transition energies ($E_{X_S^-}^b, E_{X_S^-}^d$):

$$E_{X_s^-}^b = \pm\frac{\mu_B B}{2}\left(\sqrt{(g_z^{hh}\cos\theta)^2 + (g_x^{hh}\sin\theta)^2} - \sqrt{(g_z^e\cos\theta)^2 + (g_x^e\sin\theta)^2}\right) \tag{4a}$$

$$E_{X_s^-}^d = \pm\frac{\mu_B B}{2}\left(\sqrt{(g_z^{hh}\cos\theta)^2 + (g_x^{hh}\sin\theta)^2} + \sqrt{(g_z^e\cos\theta)^2 + (g_x^e\sin\theta)^2}\right) \tag{4b}$$

The lines shown in Figs. 3(a) and 3(b) are the fits to the data using expressions (4a) and (4b) in the case of X_S^- and using Eq. (1) for X. The values utilized in the fitting of the X_S^- data were $g_z^e = (0.20 \pm 0.05)$, $g_x^e = (0.2 \pm 0.1)$, $g_z^{hh} = (-1.85 \pm 0.05)$, and $g_x^{hh} = (0.0 \pm 0.1)$. In the case of the X the parameters obtained were $\delta_o = (157 \pm 9)$ μeV, $g_z^e = (0.20 \pm 0.05)$, $g_x^e = (0.2 \pm 0.1)$, $g_z^{hh} = (-2.00 \pm 0.05)$, and $g_x^{hh} = (0.0 \pm 0.1)$. The absence of exchange splitting for X_S^- becomes evident when plotting the difference between the average of the dark-related states and the average of the bright-related states. This is shown in Fig. 3(c) for the case

of X (open symbols) and X_S^- (solid symbols) for several values of θ. We find that δ_o is large and independent of θ for the exciton, and approximately zero, within our experimental error, for the X_S^- transition. From these fittings we observed that the g factors of both excitons and trions are the same which indicates that the g-factor corrections due to electron-electron interaction are negligible.

We also note that there is a set of transitions at energies higher than X that behave like trions from their temperature dependence [Fig. 2(a)]. These transitions are below the first PL excitation resonance of X by $\sim$1.3 meV. However, their exchange energies, as measured in the Voigt geometry, are two-thirds that of the exciton, and thus they behave neither like an exciton nor like the trion singlet. We tentatively attribute these transitions to triplet states, but further experiments are necessary for a full identification. This assignment is complicated by the fact that the triplet states should be associated with excited QD states, which vary strongly from dot to dot.

To conclude, we have been able to study the evolution of the X^- from the quantum well into the QD regime, in which lateral potential steps with magnitudes up to tens of meV lead to quantum confinement of the trion. This system and this study provide an interesting point of contact between the work over the last decade on the physics of trions in wider quantum wells[2–10] and the more recent studies of charged excitons in self-assembled QDs.[11] The rich single-dot magnetophotoluminescence spectra obtained for both the X^- and X provide detailed information on the internal structure of these entities. Specifically, in a comparison of the fine structure of the localized exciton and trion we found that the g factors are very similar, however, the exchange splitting, observed in the case the exciton, goes to zero for the trion, as expected. The observation of all four transitions for X_S^- demonstrate the capability of mixing bright and dark related transitions, which is a prerequisite for optically controlling the spin state of the electron via the trion.[20] Furthermore, the extremely sharp linewidths combined with the highly selective excitation and detection that is possible in single trion spectroscopy open up the opportunity for wavefunction engineering of a single electronic spin, similar to what has been done with excitons,[21] but now with a long-lived ground-state coherence.

This work was supported in part by the ONR and by the DARPA/Spins program. J.G.T. is a NRC/NRL Research Associate. We thank V. Korenev, I. Merkulov, A. Efros, D. Steel, and L. Sham for enlightening discussions.

[1] M. A. Lampert, Phys. Rev. Lett. **1**, 450 (1958).
[2] K. Kheng *et al.*, Phys. Rev. Lett. **71**, 1752 (1993).
[3] G. Finkelstein *et al.*, Phys. Rev. Lett. **74**, 976 (1995).
[4] A. J. Shields *et al.*, Phys. Rev. B **51**, 18 049 (1995).
[5] D. Sanvitto *et al.*, Science **294**, 837 (2001).
[6] G. Eytan *et al.*, Phys. Rev. Lett. **81**, 1666 (1998); Y. Yayon *et al.*, Phys. Rev. B **64**, 081308 (2001).
[7] C. Riva, F. M. Peeters, and K. Varga, Phys. Rev. B **61**, 13 873 (2000).
[8] B. Stébé *et al.*, Phys. Rev. B **56**, 12 454 (1997).
[9] A. Wojs, J. J. Quinn, and P. Hawrylak, Phys. Rev. B **62**, 4630 (2000).
[10] A. B. Dzyubenko and A. Yu. Sivachenko, Phys. Rev. Lett. **84**, 4429 (2000); H. A. Nickel *et al.*, *ibid.* **88**, 056801 (2002).
[11] A. Wojs and P. Hawrylak, Phys. Rev. B **51**, 10 880 (1995); L. Landin *et al.*, Science **280**, 262 (1998); A. Hartmann *et al.*, Phys. Rev. Lett. **84**, 5648 (2000); R. J. Warburton *et al.*, Nature (London) **405**, 926 (2001); K. F. Karlsson *et al.*, Appl. Phys. Lett. **78**, 2952 (2001); D. Haft *et al.*, *ibid.* **78**, 2946 (2001); F. Findeis *et al.*, Phys. Rev. B **63**, 121309 (2001); J. J. Finley *et al.*, *ibid.* **63**, 073307 (2001); D. V. Regelman *et al.*, Phys. Rev. B **64**, 165301 (2001).
[12] D. Gammon *et al.*, Phys. Rev. Lett. **76**, 3005 (1996).
[13] M. Bayer *et al.*, Phys. Rev. B **61**, 7273 (2000).
[14] J. Puls *et al.*, Phys. Rev. B **60**, 16 303 (1999); L. Besombes, K. Kheng, and D. Martrou, Phys. Rev. Lett. **85**, 425 (2000).
[15] H. W. van Kesteren *et al.*, Phys. Rev. B **41**, 5283 (1990).
[16] E. Blackwood *et al.*, Phys. Rev. B **50**, 14 246 (1994); S. Glasberg *et al.*, *ibid.* **60**, 16 295 (1999).
[17] E. I. Ivchenko and G. E. Pikus, *Superlattices and Other Heterostructures, Symmetry and Optical Phenomena* (Springer-Verlag, Berlin, 1995).
[18] D. Gammon *et al.*, Phys. Rev. Lett. **86**, 5176 (2001).
[19] Here we have changed a sign in Eq. (2) of Ref. 23 so that the resulting exciton g factors are consistent with Refs. 20–22.
[20] Spin-flip Raman transitions have been used to probe and control the spin state of a neutral donor through its excited state, the neutral donor-bound exciton. This system is a good analog to a negative trion in a quantum dot. D. G. Thomas and J. J. Hopfield, Phys. Rev. **175**, 1021 (1968); S. Geschwind and R. Romestain, in *Light Scattering in Solids IV* (Springer-Verlag, Berlin, 1984), p. 151.
[21] N. H. Bonadeo *et al.*, Science **282**, 1473 (1998).